

# Magnetic transition in Ni-Pt alloy Systems : Experiment and Theory

Uday Kumar†, K. G. Padmalekha\*, P. K. Mukhopadhyay†‡  
Durga Paudyal\*\*§ and Abhijit Mookerjee\*\*

†Laboratory for Condensed Matter Physics, S.N. Bose National Centre for Basic Sciences, JD Block, Sector 3, Salt Lake City, Kolkata 700098, India

\*Department of Physics, Indian Institute of Science, Bangalore 560012, India

\*\* Condensed Matter Theory group, S.N. Bose National Centre for Basic Sciences, JD Block, Sector 3, Salt Lake City, Kolkata 700098, India

**Abstract.** We report here the preparation and measurements on the susceptibility, sound velocity and internal friction for Ni-Pt systems. We then compare these experimental results with the first principle theoretical predictions and show that there is reasonable agreement with experiment and theory.

PACS numbers: 71.20, 71.20c

## 1. Introduction

The Ni-Pt alloy system is an interesting study both because of earlier controversies about theoretical predictions regarding its chemical stability and its magnetic properties.

Some initial studies predicted these systems to be phase separating contradicting experimental observations. In our previous work [1, 2] we concluded that NiPt system is stable *provided* we take into account scalar relativistic corrections to the underlying Schrödinger equation and deal with both charge transfer and lattice relaxation effects properly.

For the 50% alloy there is also a disagreement regarding its magnetic properties. Early experiments indicated that disordered NiPt is ferromagnetic [3], while in the ordered phase it is paramagnetic [4]. Other authors found ordered NiPt to be antiferromagnetic [5]. Spin polarized local density approximation based calculations seem to indicate that even  $\text{Ni}_{25}\text{Pt}_{75}$  shows some local magnetic moment, whereas experiments seem to indicate that there is no magnetism at all.

In this communication we report susceptibility, sound velocity and internal friction experiments on a series of NiPt alloys with Pt concentrations varying between 41% and 76%. We have also carried out spin-polarized local-density based tight-binding linearized

† email:pkm@bose.res.in

§ email:dpaudyal@bose.res.in

muffin-tin orbitals (TB-LMTO) calculations for the magnetic properties of these alloys and analyze the experimental results in this light.

## 2. Experimental details

### 2.1. Sample preparation and characterization

We made four different compositions of the alloy,  $\text{Ni}_x\text{Pt}_{1-x}$  (in atomic percentages). First an amount of Ni was cut from an ingot of pure Ni. After weighing it, a target amount of Pt was cut from pure Pt wire. Since there would always be a little bit of error in weight adjustments, the exact target composition was never reached, but we determined the final composition to be close to it. This is tabulated in table 1.

**Table 1.** Composition analysis for the NiPt samples.

Target composition	Actual composition	Nearest whole number composition	Lattice Constants in nm
$\text{Ni}_{60}\text{Pt}_{40}$	$\text{Ni}_{58.7}\text{Pt}_{41.3}$	$\text{Ni}_{59}\text{Pt}_{41}$	0.372
$\text{Ni}_{50}\text{Pt}_{50}$	$\text{Ni}_{49.6}\text{Pt}_{50.4}$	$\text{Ni}_{50}\text{Pt}_{50}$	0.376
$\text{Ni}_{45}\text{Pt}_{55}$	$\text{Ni}_{44.6}\text{Pt}_{55.4}$	$\text{Ni}_{45}\text{Pt}_{55}$	0.377
$\text{Ni}_{25}\text{Pt}_{75}$	$\text{Ni}_{23.9}\text{Pt}_{76.1}$	$\text{Ni}_{24}\text{Pt}_{76}$	0.384

The materials for the required composition were then put in an arc furnace and melted in a flowing argon atmosphere. After melting, the mass formed into a shinning button. We measured the maximum mass loss to be 0.8%. These are now taken out and initial homogenizations were done under sealed and evacuated quartz ampoules at 1000°C for 12 hours. Then they were quenched to room temperature. Afterwards they were carefully cold rolled to about 0.5mm thickness and cut into reed shapes.

The samples are then again put in evacuated quartz ampules and heat treated to 1000° C for 72 hours. After quenching, they were finally annealed at 200° C for 4 hours to remove the stresses due to thermal shock that develops due to fast quenching.

The crystal structures of the samples were then measured in a standard XRD instrument (Philips make). Scans were taken from 4° to 90° at an interval of 0.02° with a step time of 0.5 sec. Diffractograms for the samples are shown in figure 1.

The analysis of the XRD data indicate that all the samples have signatures of the face centered cubic (fcc) structure. If the alloy was ordered, it would have showed the signatures of the L10, L12 or other relevant superstructures. We do not see any indication of that. This implies that all the samples were probably in the disordered phase which is expected because of homogenization at and quenching from 1000° C. There is good agreement between our experimental lattice parameters and that of Parra *et al* [3].

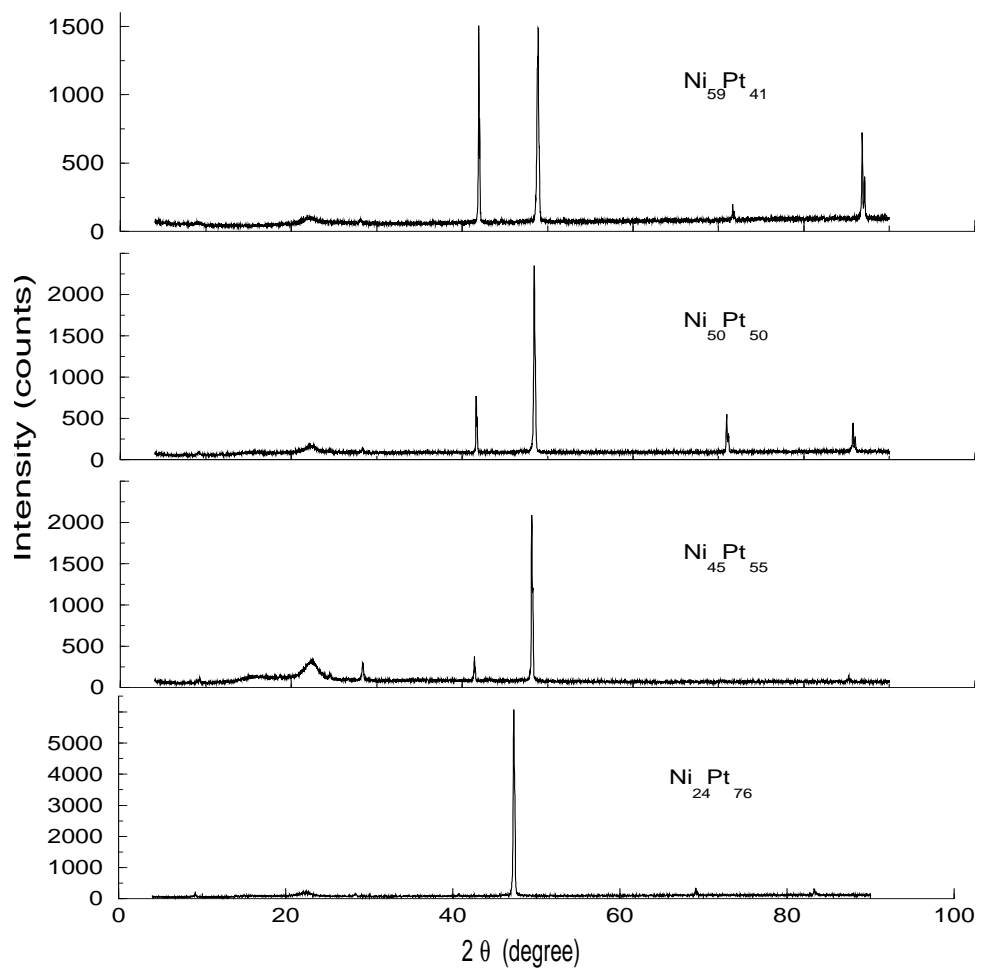


Figure 1. XRD for NiPt systems

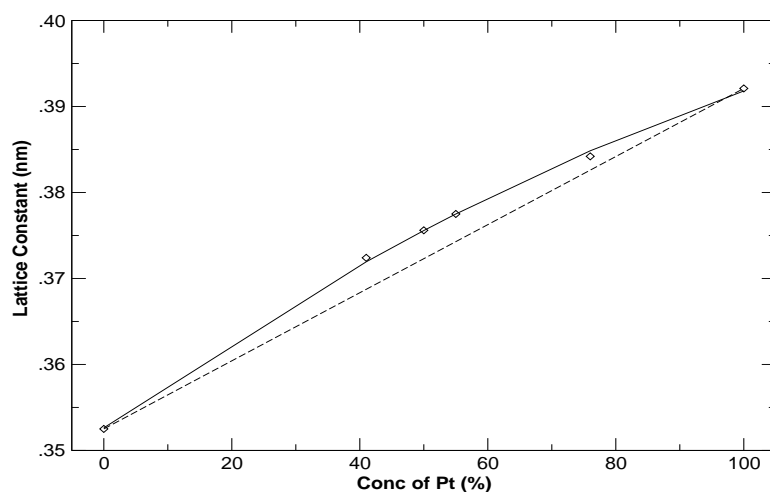
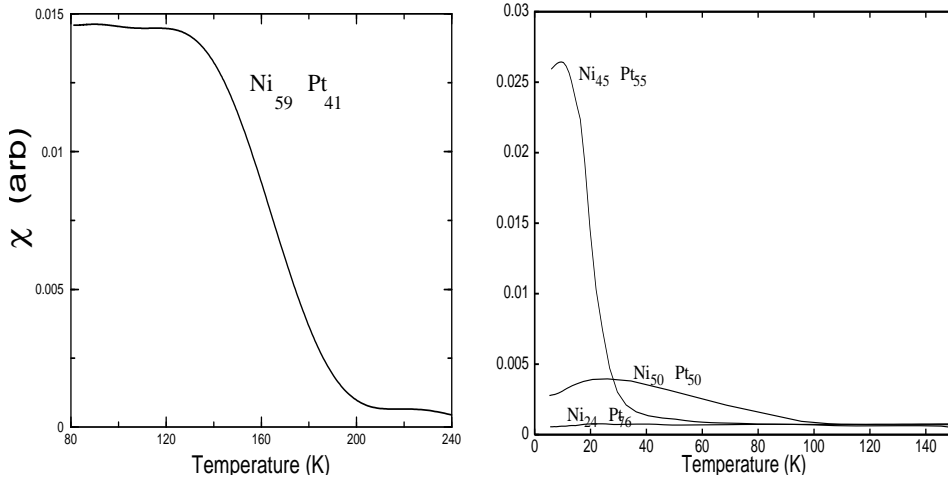


Figure 2. Deviations from Vegard's Law (dashed lines)



**Figure 3.** Susceptibility curve for NiPt with (left) 41% Pt and (right) 50%, 55% and 76% Pt

The figure 2 shows the lattice constants as a function of the Pt concentration. The figure clearly shows deviations from Vegard's Law and a positive 'bowing' effect. This is to be expected because of the large size mismatch between Ni and Pt atoms. The maximum deviation occurs at around the 50% concentration.

## 2.2. Susceptibility measurements

In figure 3 we show the data for the susceptibilities of the four samples. All except

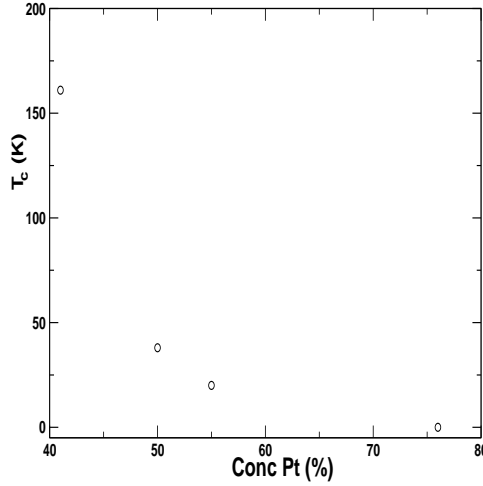


**Figure 4.** Experimental Curie temperature *vs* the alloy composition

for  $\text{Ni}_{59}\text{Pt}_{41}$  were done till liquid helium temperature. The measurements were done in a standard double balanced coil technique. Driving field was about 100 Oe and frequency was 120 Hz for the three samples, whereas for  $\text{Ni}_{59}\text{Pt}_{41}$  it was 33 Hz. Taking  $T_c$  to be

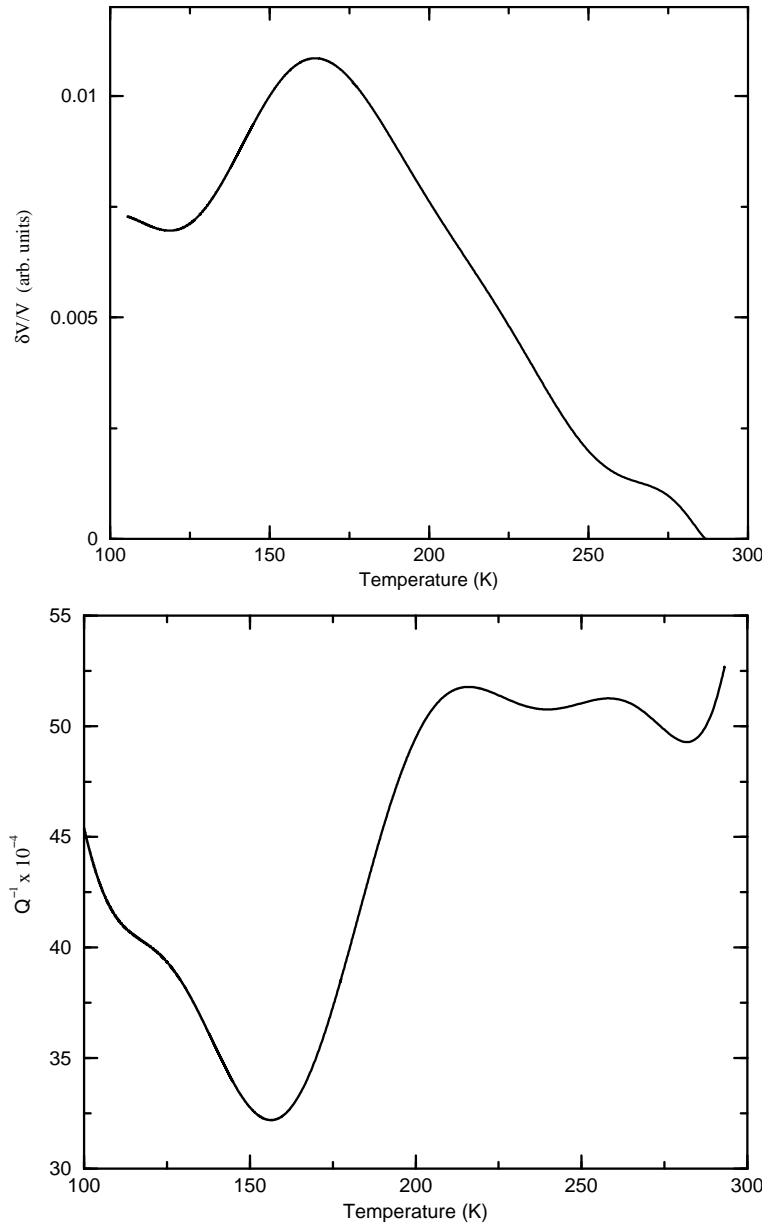


**Figure 5.** (Top) Sound velocity and (Bottom) Internal friction for  $\text{Ni}_{59}\text{Pt}_{41}$

the temperature where  $\partial\chi/\partial T$  shows a maximum, we find that for  $\text{Ni}_{59}\text{Pt}_{41}$   $T_c$  is around 161K. We summarize the various  $T_c$ s in figure 4.

### 2.3. Sound velocity and attenuation

In this section we describe the sound velocity and internal friction ( $Q^{-1}$ ) measurements done on the systems as a function of temperature. However, since the present setup does not reach below about 77K, data for only the  $\text{Ni}_{59}\text{Pt}_{41}$  are shown in figure 5. The top figure shows the sound velocity results and the bottom one shows the internal friction data. In this case we could measure to temperature lower than  $T_c$ .

These measurements are done by the vibrating reed technique. For this the sample

was taken in the form of a reed and clamped at one end in the sample holder. The free end was made to resonate by electrostatic drive from one driver electrode placed near one surface there. Another electrode at the opposite side picked up this signal and fed to a lock-in amplifier (LIA). This LIA was run at 2f mode from the reference provided by the signal generator for the driver. An integrator completed the phase locked loop that was setup to track the changes in resonance characteristics of the sample as the temperature was varied. The temperature was measured with the help of a platinum resistance thermometer. Detailed description of the vibrating reed technique can be found in [6].

From figure 5 (top), we see that as the temperature was lowered, initially the sound velocity was increasing. However, as the temperature approached  $T_c$ , the lattice softened up and the sound velocity showed a good amount of drop. However, for  $T$  far below  $T_c$ , the sound velocity again picked up, signaling the end of the magnetic transition and returned to the background lattice elastic limit. In case of internal friction (figure 5, bottom), we see an exactly complementary behaviour. Here the general lowering of  $Q^{-1}$  was enhanced as  $T$  approached  $T_c$ , till it dropped to about 50% of the room temperature value. And just like the sound velocity, it tended to recover to a general lower value at still lower temperatures.

Both these elastic measurements show that with the onset of magnetic transition, the background lattice elastic properties get largely modified due to strong spin lattice coupling in this system. In case of sound velocity which is the real part of elasticity, the elastic modulus fell to about 50% across the transition. The peak temperature,  $T_p$ , is about 161K which is about the same as the  $T_c$  as determined from the real part of  $\chi$ . However, it is well known that the effect of ferromagnetism on spin lattice coupling can start from a little below  $2T_c$  [7, 8], we actually see that the sound velocity started a faster rise below around 260K. The same argument predicts reduction of effect of magnetic transition down from  $T_c/2$  and it is also seen in the recovery of sound velocity.

In the similar vein, we can see the effect of magnetic transition on  $Q^{-1}$  data too. We see that the general fall of  $Q^{-1}$  was arrested below 250K and a massive fall in it occurred. The minimum temperature,  $T_m$ , is about 158K – below  $T_p$ . Again this is well documented [7] that  $T_m$  (determined from the imaginary part) always lags behind  $T_p$  (determined from the real part). And just like the real part,  $Q^{-1}$  also recovered from the effects of magnetic transition below about  $T_c/2$ . Hence we find that the effect of magnetic transition was to both soften the lattice and also reduce the anharmonicity of it simultaneously. We could have tried to fit a general elastic background to the data and extract the magnetic part from it. However, there are major problems in it. We need to have data from much above  $2T_c$  to much below  $T_c/2$  – which are not available. And in any case the fittings are always ambiguous and subject to intense debate. So we would not like to do it here.

### 3. Theoretical and Computational methods

For a theoretical estimation of the Curie temperatures we have followed two different approaches. In the first method, we calculate the magnetic pair energies and then use the mean field approximation to evaluate the approximate Curie temperatures. For magnetic pair interaction energies we embed different atoms with their accompanying spins in an averaged non-magnetic disordered medium at two different sites a distance  $R$  apart. The pair interactions are defined as :

$$\begin{aligned} J_{AA}(R) &= E_{AA}^{\uparrow\uparrow} + E_{AA}^{\downarrow\downarrow} - E_{AA}^{\uparrow\downarrow} - E_{AA}^{\downarrow\uparrow} \\ J_{BB}(R) &= E_{BB}^{\uparrow\uparrow} + E_{BB}^{\downarrow\downarrow} - E_{BB}^{\uparrow\downarrow} - E_{BB}^{\downarrow\uparrow} \\ J_{AB}(R) &= E_{AB}^{\uparrow\uparrow} + E_{AB}^{\downarrow\downarrow} - E_{AB}^{\uparrow\downarrow} - E_{AB}^{\downarrow\uparrow} \end{aligned}$$

We obtain these pair interactions directly using the orbital peeling technique [9] in conjunction with the augmented space recursion [10] introduced by us earlier in a tight-binding linearized muffin-tin orbitals basis (TB-LMTO) [11].

Using these interaction energies the Bragg-Williams mean-field expression for Curie temperature is

$$T_c = \frac{1}{k_B} \left[ -x^2 J_{AA} - (1-x)^2 J_{BB} + 2x(1-x) J_{AB} \right]$$

$$J_{AA} = \sum_R J_{AA}(R) \text{ etc.}$$

The other approach is the Mohn-Wohlfarth (MW) procedure [12] :

$$\left( \frac{T_C}{T_S} \right)^2 + \frac{T_C}{T_{SF}} - 1 = 0$$

where,  $T_S$  is the Stoner temperature calculated from the relation

$$\langle I(E_F) \rangle \int_{-\infty}^{\infty} dE N(E) \left( \frac{\partial f}{\partial E} \right) = 1$$

$\langle I(E_F) \rangle$  is the concentration averaged Stoner parameter ,  $N(E)$  is the density of states per atom per spin of the paramagnetic state [13] and  $f(E)$  is the Fermi distribution function. The spin fluctuation temperature  $T_{SF}$  is given by,

$$T_{SF} = \frac{m^2}{10k_B \langle \chi_0 \rangle}$$

$\langle \chi_0 \rangle$  is the concentration weighted exchange enhanced spin susceptibility at equilibrium and  $m$  is the averaged magnetic moment per atom.  $\chi_0$  is calculated using the relation by Mohn [12] and Gersdorf [14]:

$$\chi_0^{-1} = \frac{1}{2\mu_B^2} \left( \frac{1}{2N^{\uparrow}(E_F)} + \frac{1}{2N^{\downarrow}(E_F)} - I \right)$$

$N^{\uparrow}(E_F)$  and  $N^{\downarrow}(E_F)$  are the spin-up and spin-down partial density of states per atom at the Fermi level for each species in the alloy.

Alloy Composition	Lattice Constant (nm)
Ni <sub>60</sub> Pt <sub>40</sub>	0.372
Ni <sub>50</sub> Pt <sub>50</sub>	0.376
Ni <sub>45</sub> Pt <sub>55</sub>	0.378
Ni <sub>25</sub> Pt <sub>75</sub>	0.384

**Table 2.** Equilibrium lattice constants in nm

### 3.1. Lattice Structure

As shown in the table 2 and in comparison with table 1, our measured values of lattice parameters match well with the previously measured lattice parameters. In all concentrations we have got the FCC structures as par with the previous experiment by Parra *et al* [3]. It should be noted that our calculations show that for the ordered 50% alloy, the structure with a small tetragonal distortion has the lowest energy. The experimental lack of signature of any tetragonal distortion for the 50% alloy further strengthens our belief that the alloy was indeed disordered.

### 3.2. Curie Temperature

The experimental measurements in NiPt alloys with 40%, 50% and 55% concentration of Pt show the ferromagnetic to paramagnetic transitions are at 161, 38 and 20K.

Experimentally we find that the alloys up to 55% Pt do show ferromagnetic behaviour, certainly in the disordered phase. However, at 76% of Pt the alloy becomes non-magnetic. Our first principles calculations agree with this up to 55% of Pt. However, our theoretical calculations indicate that ferromagnetism persists even at 75% of Pt. We are unable to explain why this should be and why the Stoner-like arguments fail in these compositions. Table 3 shows that the Mohn-Wohlfarth and Bragg-Williams approaches both give qualitatively the correct trend in  $T_c$  up to 55% of Pt. Both approaches show the 50% alloy to be ferromagnetic, settling an earlier dispute. It is interesting to note that if we do not take into account local lattice distortion due to size mismatch in the NiPt alloys, the 50% alloy yields a Curie temperature of 76K which is quantitatively at variance with experiment. We have included size mismatch effects within our TB-LMTO-Augmented Space Recursion.

## 4. Conclusions

In this communication we have reported structural and magnetic properties of NiPt alloys. The structure was probed by XRD experiments, while the magnetic properties were probed by susceptibility, sound velocity and attenuation. Our experimental findings of lattice parameters agree with earlier experiments and confirm that our

**Table 3.** Curie temperatures in Ni-Pt alloys.

Composition	Experiment	Theory I (Mohn-Wohlfarth)	Theory II (Bragg-Williams)
Ni <sub>60</sub> Pt <sub>40</sub>	161	125	232
Ni <sub>50</sub> Pt <sub>50</sub>	38	38	40
Ni <sub>45</sub> Pt <sub>55</sub>	20	35	17

samples were in the disordered state. We have also carried out a theoretical study of the same alloy system and compared the theoretical predictions with the experimental results. The theory correctly predicts the trend in the Curie temperature. The Ni<sub>50</sub>Pt<sub>50</sub> alloy was found to be ferromagnetic, settling an earlier dispute. Our theory cannot explain why ferromagnetism disappears around the Ni<sub>25</sub>Pt<sub>75</sub> composition.

### Acknowledgments

We would like to thank Drs. A. Mitra and P. K. De for the samples, Prof. A.K. Majumder for the use of his arc furnace and Prof. A.K. Raychaudhuri for measurement till 5K. We would also like to thank Dr. D. Das for his various helps at critical stages and Mr. S. Chanda for help in rolling the samples. We would like to thank Mr. D. Hazra for his help with XRD analysis. We would like to acknowledge partial support from TWAS under its project grant 97-212 RG/PHYS/AS and the CSIR project grant 03(948)/02-EMR-II.

### References

- [1] D. Paudyal, T. Saha-Dasgupta, A. Mookerjee, J. Phys.: Condens. Matter 15 (2003) 1029
- [2] D. Paudyal, T. Saha-Dasgupta, A. Mookerjee, J. Phys.: Condens. Matter 16 (2004) 2317
- [3] R.E. Parra, J.W. Cable, Phys. Rev. B 21 (1980) 5494
- [4] C.E. Dahmani, M.C. Cadeville, J.M. Sanchez, J.L. Moran-Lopez, Phys. Rev. Lett. 55 (1985) 1208
- [5] J.B. Staunton, B.L. Gyorffy, D.D. Johnson, F.J. Pinski, G.M. Stocks in: V. Kumar, O.K. Andersen and A. Mookerjee (Eds.), Proceedings of Miniworkshop on electronic structure calculations and working group on disordered alloys, World Scientific, (1994)
- [6] P. K. Mukhopadhyay, A. K. Raychaudhuri, J. Phys. E: Sci. Instrum. 20 (1987) 507
- [7] P. K. Mukhopadhyay, A. K. Raychaudhuri, J. Phys. C: Solid State Phys. 21 (1988) L385
- [8] P. K. Mukhopadhyay, A.K. Raychaudhuri, Journal of Applied Physics 67 (1990) 5235
- [9] N.R. Burke, Surface Sci. 58 (1976) 349
- [10] T. Saha, I. Dasgupta, A. Mookerjee, Phys. Rev. B 50 (1994) 13267
- [11] O. K. Andersen, O. Jepsen, Phys. Rev. Lett. 53 (1984) 2581
- [12] P. H. Mohn, E. P. Wohlfarth, J. Phys. F: Met. Phys. 17 (1987) 2421
- [13] O. Gunnarsson, J. Phys. F: Met. Phys. 6 (1976) 587
- [14] R. Gersdorf, J. Phys. Radium 23 (1962) 726